Applied Catalysis B: Environmental 301 (2022) 120784

Contents lists available at ScienceDirect

Applied Catalysis B: Environmental

journal homepage: www.elsevier.com/locate/apcatb

Effects of SO_2 on standard and fast SCR over $CeWO_x$: A quantitative study of the reaction pathway and active sites

Yanlong Huo [a,b], Kuo Liu [a,d,*], Jingjing Liu [a], Hong He [a,b,c,*]

[a] State Key Joint Laboratory of Environment Simulation and Pollution Control, Research Center for Eco-Environmental Sciences, Chinese Academy of Sciences, Beijing 100085, China
[b] University of Chinese Academy of Sciences, Beijing 100049, China
[c] Center for Excellence in Regional Atmospheric Environment, Institute of Urban Environment, Chinese Academy of Sciences, Xiamen 361021, China
[d] Editorial Office of Journal of Environmental Sciences, Research Center for Eco-Environmental Sciences, Chinese Academy of Sciences, Beijing 100085, China

ARTICLE INFO

Keywords:
Mechanism
SO_2
$CeWO_x$
Standard and fast SCR
NH_4HSO_4

ABSTRACT

The influence of SO_2 on the amounts of NO_2, NH_3 and NO adsorbed on $CeWO_x$ and the reaction pathway of fast and standard SCR were investigated using transient reaction experiments and in situ DRIFTS. The negative effect of SO_2 was less severe during fast SCR. The SO_2 adsorption inhibited NO adsorption and the "nitrite path", which is detrimental for standard SCR at low temperatures. For fast SCR, although "nitrite path" and "NH_4NO_3 path" were inhibited, the greater amount of nitrates from NO_2 adsorption, acceleration of NH_4HSO_4 decomposition, and promoted reaction between the NO gas, surface nitrates and adsorbed NH_3 made the inhibitory effect of SO_2 less severe. Brønsted acid sites are more active and make the main contribution to SCR with SO_2. NH_4HSO_4 may not be the main cause of deactivation. When H_2O and SO_2 were present, "nitrite path" was seriously inhibited and "NH_4NO_3 path" was absent, causing decreased activity.

1. Introduction

Nitrogen oxides (NO_x) in the atmosphere, which are important pollutants, can cause serious environmental problems and have biological toxicity [1]. Diesel vehicles contribute the majority of NO_x emissions, so controlling their exhaust emission is a top priority [2,3]. Selective catalytic reduction (SCR) with NH_3 is the mainstream technology for NO_x treatment, and V_2O_5-WO_3/TiO_2 has been widely used in NH_3-SCR because of its high SCR activity and resistance to sulfur poisoning [4–6]. However, traditional V-based catalysts have several disadvantages, including toxicity, a narrow temperature window, and poor selectivity at high temperature [7–9]. A $CeWO_x$ catalyst prepared by Shan et al. [2] with the urea homogeneous precipitation method could exhibit 100% conversion in the temperature range of 250–425 °C at a high space velocity of 500, 000 h^{-1}, and is promising for application in NO_x reduction. Due to the presence of SO_2 in the exhaust gas, the catalyst is required to exhibit excellent sulfur poisoning resistance [10]. However, comprehensive studies on the effects of SO_2 on this $CeWO_x$ catalyst are still lacking.

In the presence of SO_2, NH_3-SCR catalysts are often deactivated, especially at low temperatures below 250 °C. Some studies show that the presence of SO_2 mainly inhibits the formation of nitrate and blocks the Langmuir-Hinshelwood (L-H) path at low temperatures below 200 °C [11]. In addition, ammonium sulfate or ammonium bisulfate deposit on the surface of the catalyst, blocking the active sites of the catalyst [7,12]. At higher temperatures, e.g. at 300 °C, Xu et al. [13] pointed out that Ce$(SO_4)_2$ and $Ce_2(SO_4)_3$ with high thermal stability are formed by the reaction between SO_2 and Ce, destroying the redox transformation between Ce(IV) and Ce(III), inhibiting the formation of nitrate, and deactivating the Ce/TiO_2 catalyst. Until now, most studies have applied qualitative determination methods, e.g. in situ diffuse reflectance infrared Fourier transform spectroscopy (DRIFTS) [7,11,14] or X-ray photoelectron spectroscopy (XPS) [15,16], in clarifying the effect of SO_2; however, quantitative information on NO_x and NH_3 adsorption on Ce-based catalysts in the presence of SO_2 has not been reported.

Fast SCR involving equal amounts of NO_2 and NO has been reported to be many times faster than standard SCR, especially at low temperatures [17–19]. So far, few researchers have focused on the behavior of NH_3-SCR catalysts during fast SCR in the presence of SO_2. On V_2O_5-WO_3/TiO_2, NH_4HSO_4 decomposes faster in NO/NO_2 than in a NO atmosphere. The promotional effect of NO_2 was ascribed to the faster

* Corresponding authors at: State Key Joint Laboratory of Environment Simulation and Pollution Control, Research Center for Eco-Environmental Sciences, Chinese Academy of Sciences, Beijing 100085, China.
E-mail addresses: kuoliu@rcees.ac.cn (K. Liu), honghe@rcees.ac.cn (H. He).

https://doi.org/10.1016/j.apcatb.2021.120784
Received 23 June 2021; Received in revised form 4 September 2021; Accepted 29 September 2021
Available online 1 October 2021

reoxidation of the reduced V species by NO_2 acting as an oxidizing agent, leading to faster reaction between NO/O_2 and ammonium bisulfate [4,12,20]. However, studies on the effects of SO_2 on fast SCR over Ce-based catalysts are still lacking.

Acid sites have been reported to be important during NH_3-SCR on some NH_3-SCR catalysts, but which kind of acid sites is more active is still controversial. Some researchers found that NH_3 species activated on Lewis acid sites reacted faster than those on Brønsted acid sites on V_2O_5/TiO_2 and V_2O_5-WO_3/TiO_2 [5,21,22]. On the other hand, some researchers reported that NH_3 on Brønsted acid sites is more active, e.g. on vanadia/titania [23]. Interconversion between Lewis and Brønsted acid sites might also be present, and Lewis acid sites can be hydrolyzed, e.g. on W-substituted vanadium oxide [24]. Also, the number of Brønsted acid sites increases after the pretreatment of the catalysts, e.g., CeO_2 cubes [8] and $Ce_{0.3}TiO_x$ [11], by SO_2 gas. Until now, few studies have clarified which kind of acid site is more active for NH_3-SCR on Ce-based catalysts, especially during fast SCR or in the presence of SO_2.

In this study, the adsorption capacity for SO_2 and the effect of SO_2 on the amounts of NO, NO_2 and NH_3 adsorbed were quantitatively determined, and the mechanisms of H_2O and SO_2 inhibition on the NH_3-SCR reaction pathway were also studied. The contributions of Brønsted and Lewis acid sites on the $CeWO_x$ surface to NH_3-SCR in the presence of SO_2 were obtained. The results can provide guidance for the synthesis of sulfur-resistant catalysts.

2. Experimental methods

2.1. Catalyst preparation and activity tests

The $CeWO_x$ catalyst (Ce/W molar ratio 1:1) was synthesized using a homogeneous precipitation method [2]. 40–60 mesh $CeWO_x$ was applied in the activity test and adsorption experiments. The SCR activity was measured in a quartz flow reactor with a total flow rate of 500 mL min^{-1} and a gas hourly space velocity (GHSV) of 300,000 h^{-1}. The composition of the gas was 5 vol% O_2, 500 ppm NH_3, 500 ppm NO for standard SCR, 250 ppm NO_2 + 250 ppm NO for fast SCR, 100 ppm SO_2 (when used), 5 vol% H_2O (when used) and N_2 as the balance gas. The composition of the product gases, including N_2O, NH_3, NO, and NO_2, was analyzed by an online NEXUS 670-FTIR spectrometer according to the previous report [25]. The NO_x conversion and N_2 selectivity were obtained according to the equations:

$$NO_x\text{conversion} = \left(1 - \frac{[NO]_{out} + [NO_2]_{out}}{[NO]_{in} + [NO_2]_{in}}\right) \times 100\%$$

$$N_2\ \text{selectivity} = \left(1 - \frac{2[N_2O]_{out}}{[NO_x]_{in} + [NH_3]_{in} - [NO_x]_{out} - [NH_3]_{out}}\right) \times 100\%$$

2.2. Quantification and characterization

A transient response method (TRM) was used to quantitatively study the adsorption capacity of $CeWO_x$ for the reactants (SO_2, NO, NO_2 and NH_3) at 30 and 200 °C. The experimental setup and the measuring principle were described in our previous study [25]. The concentrations of SO_2, N_2O, NH_3, NO, and NO_2 were analyzed by an online NEXUS 670-FTIR spectrometer [25]. 100 mg $CeWO_x$ was pretreated in 20 vol% O_2/N_2 for 30 min at 400 °C. The adsorption gases were 2 vol% H_2O, 100 ppm SO_2, 500 ppm NO, 500 ppm NO_2, or 500 ppm NH_3 with N_2 balance. After the pretreatment of $CeWO_x$ in different atmospheres at 30 °C, temperature programmed surface reaction (TPSR) (heating rate 10 °C min^{-1}) was carried out in 500 ppm NO/N_2 or (100 ppm SO_2 + 500 ppm NO)/N_2 or (100 ppm SO_2 + 500 ppm NO + 2 vol% H_2O)/N_2 from 30 °C to 400 °C with a total gas flow rate of 500 mL min^{-1}. The pretreatment conditions prior to TPSR are described in detail in Supporting information (Section S1.1).

The experiments of in situ DRIFTS were conducted on an FTIR spectrometer (Nicolet IS50) with a MCT/A detector which was cooled by liquid nitrogen. Firstly, the sample was pretreated at 400 °C for 30 min by 20 vol% O_2/N_2, then cooled to 30 or 200 °C and purged with N_2. After accumulating 50 scans, the spectra were recorded, with a resolution 4 cm^{-1}. The gas flow rate was 250 mL min^{-1} and the gases were 100 ppm SO_2 or 500 ppm NO_2, with N_2 balance.

3. Results and discussion

3.1. Influence of SO_2 on the activity of $CeWO_x$

The activity tests were conducted at 200 °C when ammonium bisulfate or ammonium sulfate was present and at 300 °C when ammonium bisulfate or ammonium sulfate decomposed [11,26]. Fig. 1 depicts the stability of $CeWO_x$ and N_2 selectivity in the presence of SO_2 at 200 °C and 300 °C during standard and fast SCR. N_2 selectivity was > 99% during both standard and fast SCR at either 200 or 300 °C (Fig. 1**b**), and the concentration of N_2O formed was quite low (Fig. S1b). Without SO_2 and H_2O, NO_x conversion could be maintained at about 64% and 98% during standard and fast SCR at 200 °C, respectively. During standard SCR, when 100 ppm SO_2 was fed into the reactor, the NO_x conversion rate decreased rapidly in the first hour, and then slowly decreased to 20% in the next 3 h. When 5 vol% H_2O and 100 ppm SO_2 were simultaneously introduced into the reactor, the NO_x conversion decreased rapidly and remained at about 4%. During fast SCR, the introduction of SO_2 caused a slight decrease in NO_x conversion, and the

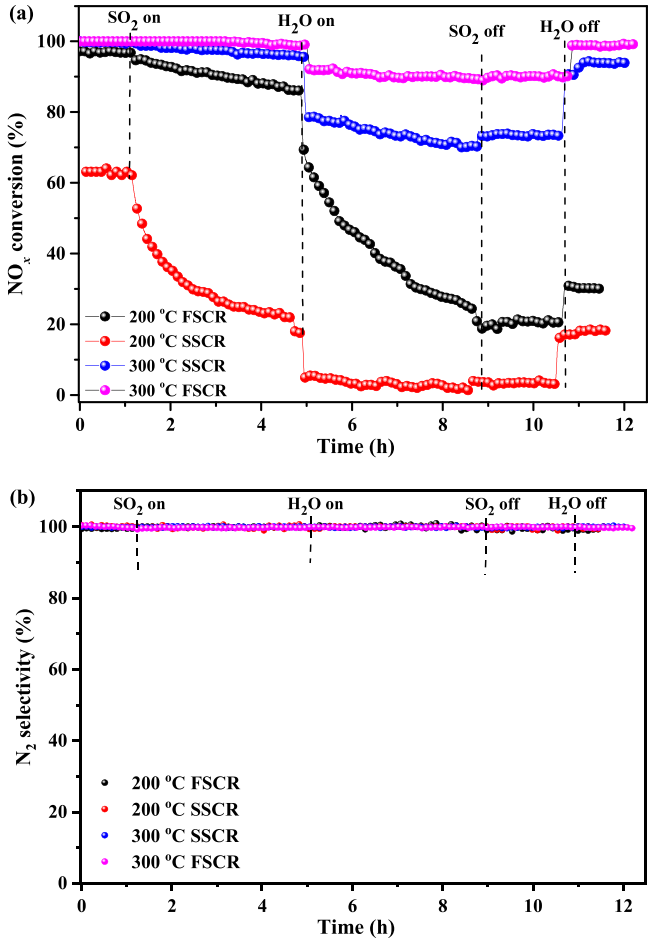

Fig. 1. (a) NO_x conversion and (b) N_2 selectivity during standard SCR (SSCR) and fast SCR (FSCR) vs. time-on-stream in the presence of SO_2/H_2O on the $CeWO_x$ catalyst at 200 and 300 °C.

subsequent addition of H_2O led to a dramatic decline in NO_x conversion. The poisonous effect of SO_2 was more severe during standard SCR than fast SCR. The better stability during fast SCR on $CeWO_x$ correlated closely with the presence of NO_2. The NO_x conversion did not change when SO_2 was removed and only slightly increased when SO_2 and H_2O were both removed from the reactant feed gases. These results indicate that SO_2 and H_2O have a detrimental and irreversible poisoning effect on $CeWO_x$ at 200 °C. The NH_3 conversion during NH_3 oxidation in the presence of SO_2 was low at 200 and 300 °C (Fig. S1c), demonstrating that the contribution of NH_3 oxidation was negligible in this study. However, at a higher temperature of 300 °C, the NO_x conversion during standard and fast SCR could be recovered to a certain extent when SO_2 and H_2O were both removed, suggesting that the detrimental effects of SO_2 and H_2O are more severe at lower temperatures. Therefore, this study mainly focused on the influence of SO_2 at the low temperature of 200 °C.

3.2. Adsorption of SO_2

As shown in Fig. 2**a**, the amounts of SO_2 consumption on fresh $CeWO_x$ were ~30 μmol g^{-1} and ~21 μmol g^{-1} at 30 °C and 200 °C, respectively. The amounts of weakly adsorbed SO_2 molecules were ~7 μmol g^{-1} at 30 °C and negligible at 200 °C (Fig. S2), hence there was some weakly adsorbed SO_2 at 30 °C. To investigate the interaction between SO_2 and the catalyst and surface products, in situ DRIFTS studies were applied. Fig. 2**b** shows the DRIFT spectra of $CeWO_x$ as a function of time in a flow of SO_2 at 30 °C. According to other studies, the peak at 1147 cm^{-1} with shoulders at 1058 and 1233 cm^{-1} [14] was attributed to sulfate species. The band at 1437 cm^{-1} [11,27] was attributed to sulfite (SO_3^{2-}) species. The band at 1327 cm^{-1} was assigned to physically adsorbed SO_2, and gradually disappeared when the sample was purged with N_2 [28]. The appearance of the bands at 1626 and 1681 cm^{-1} ascribed to adsorbed H_2O (H_2O_{ad}) means that SO_2 can react with surface hydroxyl groups through Eq. (3) [7,29]. Similarly, sulfate species were found on SO_2-adsorbed $CeWO_x$ at 200 °C, showing bands at 1136 cm^{-1}, 1361 cm^{-1} [14] and 1282 cm^{-1} [27] (Fig. 2**c**). The band at 1421 cm^{-1} [27] was attributed to SO_3^{2-} species. Adsorbed H_2O was also observed (band at 1613 cm^{-1}). Thus, Eqs. (1)–(3) might exist [4,16, 29–32].

$$O^{2-} + SO_2 \leftrightarrow SO_3^{2-} \quad (1)$$

$$[Ce^{4+}] - O^- + SO_3^{2-} \leftrightarrow SO_4^{2-} + [Ce^{3+}] - \square \quad (2)$$

$$SO_2 + 2OH^- \leftrightarrow SO_3^{2-} + H_2O_{ad} \quad (3)$$

where $[Ce^{3+}]$-□ is an oxygen vacancy of Ce site [25].

3.3. Effect of SO_2 on NO_2 adsorption

To elucidate the impact of pre-adsorbed SO_2 on the amount of NO_2 adsorbed, NO_2 adsorption on SO_2-pretreated $CeWO_x$ was conducted at both 30 and 200 °C. No N_2O, N_2O_3, N_2O_4, or N_2O_5 was generated in the whole progress. As shown in Fig. 3**a**, after pre-adsorption of SO_2 at 30 °C, the molar ratio between the NO_2 consumed (~83 μmol g^{-1}) and the NO formed (~27 μmol g^{-1}) was about 3:1; the amount of surface nitrate species ($N_{*\text{-}NO3}$) can be calculated by the following formula [25]:

$$N_{*\text{-}NO_3} = N_{NO_2\ consumption} - N_{NO\ emission} = (83\text{-}27)\ \mu mol\ g^{-1} = 56\ \mu mol\ g^{-1}$$

where $N_{NO_2\ consumption}$ and $N_{NO\ emission}$ are the amounts of NO_2 consumed and NO formed, respectively. The weakly adsorbed nitrate was ~12 μmol g^{-1} (Fig. S3). In our previous research, the surface nitrate species generated by NO_2 adsorption on the fresh catalyst was ~60 μmol g^{-1} and the weakly adsorbed nitrate was ~5 μmol g^{-1} [25], indicating that the adsorption of SO_2 inhibited NO_2 adsorption.

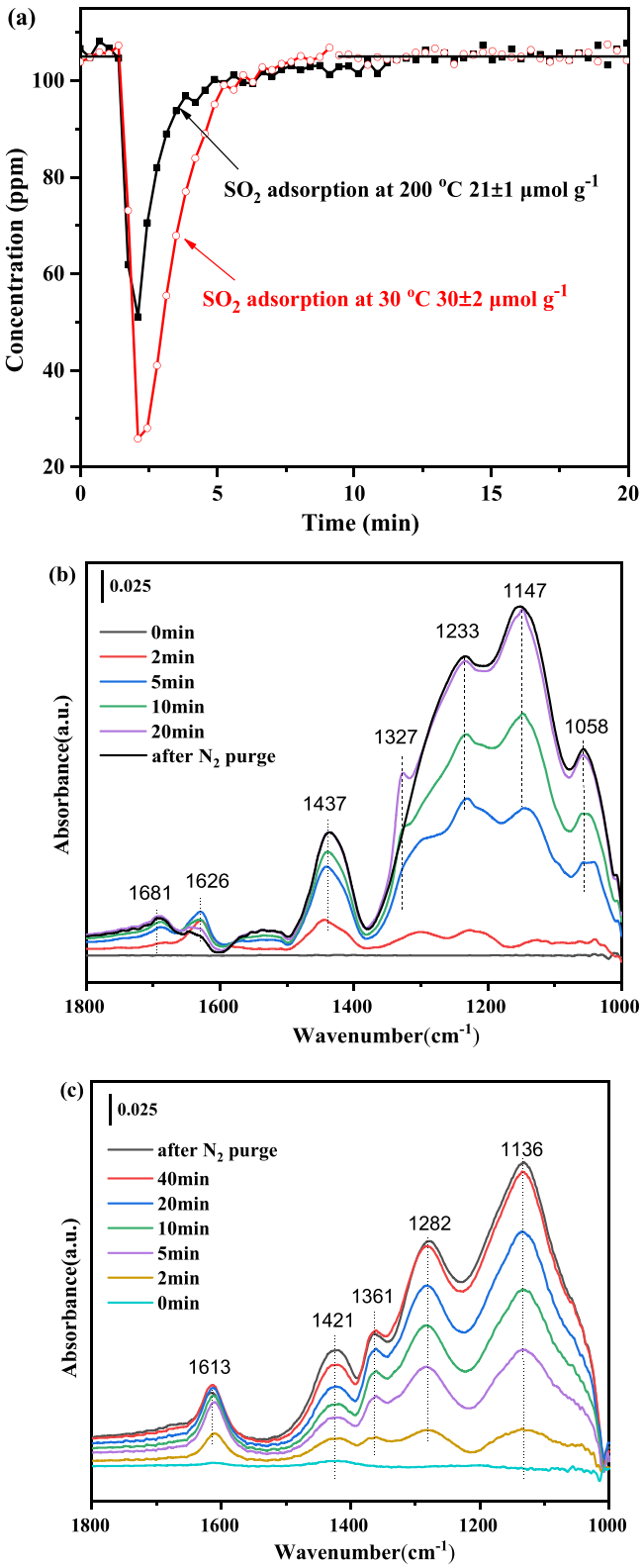

Fig. 2. Adsorption of SO_2/N_2 (100 ppm) on $CeWO_x$ at 30 and 200 °C (a). In situ DRIFTS results of $CeWO_x$ treated in flowing 100 ppm SO_2 at 30 °C (b) and at 200 °C (c).

The in situ DRIFTS results of NO_2 adsorption on the catalyst with pre-adsorbed SO_2 were also shown to explore the adsorption mechanism in more detail. As shown in Fig. 3**b**, after NO_2 adsorption at 30 °C, nitrate species were present. Based on previous studies, the bands at 1250 and

1604 cm^{-1} were ascribed to bridging nitrate [33], and the bands at 1019 and 1561 cm^{-1} were ascribed to bidentate nitrate [33]. The bands at 1278 and 1535 cm^{-1} were assigned to monodentate nitrate [28], while the band at 1454 cm^{-1} was ascribed to ionic nitrate [34]. The transformation among different nitrates took place as follows [25]:

$$[Ce^{4+}]\text{-}ONO_2\ \text{(monodentate nitrate)} + [Ce^{3+}]\text{-}\square \leftrightarrow ([Ce^{4+}]\text{-}O)_2 = NO\ \text{(bridging nitrate)} \leftrightarrow [Ce^{4+}] = O_2NO\ \text{(bidentate nintrate)} + [Ce^{3+}]\text{-}\square \quad (4)$$

The band at 1650 cm^{-1} was ascribed to adsorbed water [28], and the negative band at 3650 cm^{-1} indicates the surface hydroxyl groups were consumed. The disappearance of OH groups and evolution of H_2O may be due to the occurrence of Eqs. (7)–(9). According to the literatures [25, 35] and the in situ DRIFTS studies, we can conclude that the following reactions may occur at 30 °C:

$$2NO_2 + [Ce^{3+}]\text{-}\square \leftrightarrow [Ce^{4+}]\text{-}ONO_2 + NO \quad (5)$$

$$[Ce^{4+}]\text{-}O^- + NO_2 \leftrightarrow [Ce^{4+}]\text{-}ONO_2 \quad (6)$$

$$3NO_2 + H_2O_{ad} \leftrightarrow 2HNO_3 + NO \quad (7)$$

$$HNO_3 \leftrightarrow H^+ + NO_3^- \quad (8)$$

$$H^+ + OH^- \leftrightarrow H_2O \quad (9)$$

H_2O_{ad} originated from the adsorption of SO_2 (Fig. 2**b**). It is possible that the adsorption of SO_2 consumed some $[Ce^{3+}]$-□ sites (reverse of Eq. (2)), decreasing the NO_2 adsorption.

At 200 °C, the amount of NO_2 consumption was ~45 μmol g^{-1} on fresh $CeWO_x$ and ~22 μmol g^{-1} NO was produced at the same time (Fig. 3**a**), the amount of nitrate was 23 μmol g^{-1}. Based on our previous report [25], it can be speculated that Eq. (5) took place and the mutual transformation of nitrate (Eq. (4)) occurred. However, after pre-adsorption of SO_2 at 200 °C, the consumption of NO_2 was ~36 μmol g^{-1} and ~23 μmol g^{-1} NO was released at the same time (Fig. 3**a**). The amount of nitrate generated was calculated to be 13 μmol g^{-1}, indicating that pre-adsorbed SO_2 affects the reaction mechanism of NO_2 on $CeWO_x$ and that the sulfate and sulfite species inhibit the formation of nitrate but accelerate the formation of NO. It can be proposed that NO_2 gas could react with surface sulfate and sulfite species to form NO. To understand the effect of SO_2 on NO_2 adsorption at 200 °C, DRIFTS was carried out for the $CeWO_x$ catalyst, as depicted in Fig. 3**c**. The bands at 1609 and 1220 cm^{-1} [33] were assigned to bridging nitrate. The bands at 1018 and 1581 cm^{-1} were assigned to bidentate nitrate [33], and the band at 1520 cm^{-1} was ascribed to monodentate nitrate. The formation of different nitrates indicated the occurrence of Eq. (4), similar to that in the absence of SO_2 [25]. The peak at 1420 cm^{-1} ascribed to SO_3^{2-} decreased after the introduction of NO_2 onto the surface of $CeWO_x$, along with increases in the peaks at 1290 and 1080 cm^{-1}, which were ascribed to sulfate species [14], indicating that there was a transformation of SO_3^{2-} species to sulfate species at 200 °C. The negative peak at 1420 cm^{-1} shifted upward after 5 min and may have been affected by the nitrate absorption peak nearby. It can be inferred that the following reactions might also take place [36]:

$$SO_3^{2-} + NO_2 \leftrightarrow SO_4^{2-} + NO \quad (10)$$

At 200 °C, the presence of surface adsorbed SO_2 could convert some NO_2 to NO.

3.4. Effect of SO_2 on NH_3 adsorption

To elucidate the influence of the pre-adsorbed SO_2 on NH_3 adsorption, NH_3 adsorption on fresh, SO_2-pretreated, NO_2-pretreated and SO_2-NO_2-pretreated $CeWO_x$ was conducted. The amount of adsorbed NH_3 molecules on SO_2-saturated catalyst was ~179 μmol g^{-1} at 30 °C (Fig. 4**a**), 19 μmol g^{-1} greater than that on fresh $CeWO_x$ (~160 μmol g^{-1} [25]). According to Section 3.2, 23 μmol g^{-1} sulfate and sulfite species remained on the $CeWO_x$ surface after N_2 purging, and the amount of NH_4HSO_4 was calculated as ~19 μmol g^{-1} at 30 °C. At 200 °C, the amounts of NH_3 consumption on fresh and SO_2 saturated $CeWO_x$ were ~70 μmol g^{-1} and ~92 μmol g^{-1}, respectively (Fig. 4**a**). SO_2 increased NH_3 adsorption by 92 - 70 = 22 μmol g^{-1} at 200 °C, and the amount of adsorbed sulfate and sulfite species was 21 - 2 = 19 μmol g^{-1} after N_2 purge; hence, NH_4HSO_4 mainly formed at 200 °C. Ma et al. [37] and Tang et al. [38] proposed that NH_3, SO_3 and H_2O tend to form ammonium sulfate from the thermodynamic point of view, but this will be limited by the reaction kinetics, and the main component in the NH_3-SCR process on V_2O_5-WO_3/TiO_2 is ammonia bisulfate at 190–240 °C. In this study, the calculation results for the adsorption capacity showed that the product on the $CeWO_x$ surface was mainly NH_4HSO_4. The above in situ DRIFTS results demonstrate that adsorbed H_2O formed on the $CeWO_x$ surface during SO_2 adsorption, hence it can be speculated that Eq. (11) took place [37].

$$[Ce^{4+}]\text{-}O^- + SO_2 + NH_3 + H_2O_{ad} \leftrightarrow [Ce^{3+}]\text{-}\square + NH_4HSO_4 \quad (11)$$

Our previous study showed that nitrate and NH_3 adsorbed at different sites on the $CeWO_x$ surface, and that one molecule of NH_3 can react with one nitrate to produce NH_4NO_3 through Eq. (12) at room temperature [25].

$$[M^{n+}] - O - NH_4 + [Ce^{4+}] - ONO_2 \leftrightarrow [M^{n+}] - O - NH_4NO_3 - [Ce^{4+}] \quad (12)$$

After pre-adsorption of SO_2 and NO_2 followed by N_2 purging, ~23 μmol g^{-1} sulfate/sulfite species and ~44 μmol g^{-1} nitrate were formed on $CeWO_x$ at 30 °C. The amount of NH_3 consumption on the SO_2-NO_2-saturated catalyst was ~227 μmol g^{-1} (Fig. 4**b**), ~67 μmol g^{-1} greater than that on the fresh catalyst at 30 °C (~160 μmol g^{-1}). It can be inferred that ~44 μmol g^{-1} NH_4NO_3 formed on the surface, and ~23 μmol g^{-1} sulfate/sulfite species can react with 67 - 44 = 23 μmol g^{-1} NH_3 to form ~23 μmol g^{-1} NH_4HSO_4 at 30 °C. The weakly adsorbed NH_3 could be obtained by re-adsorption after purging with N_2, giving a value of ~78 μmol g^{-1} at 30 °C (Fig. S4), higher than that for $CeWO_x$ without adsorption of SO_2 (~59 μmol g^{-1}) [25], indicating that the presence of sulfate and sulfite species on $CeWO_x$ would weaken NH_3 adsorption.

At 200 °C, the amount of the NH_3 consumption increased from 70 μmol g^{-1} (fresh $CeWO_x$) to ~93 μmol g^{-1} (pretreated by NO_2) (Fig. 4**b**), indicating that the surface nitrates (~23 μmol g^{-1}) increased the amount of NH_3 adsorbed through producing NH_4NO_3 (Eq. (12)). As shown in Fig. 4**b**, the amount of NH_3 consumption on the SO_2-NO_2-pretreated catalyst was ~103 μmol g^{-1}, ~33 μmol g^{-1} greater than that on the fresh catalyst at 200 °C. After pre-adsorption of SO_2 and NO_2, the amounts of the sulfate/sulfite species and nitrate were ~19 μmol g^{-1} and ~13 μmol g^{-1}, respectively. Hence it is inferred that ~19 μmol g^{-1} NH_4HSO_4 and ~13 μmol g^{-1} NH_4NO_3 existed on the $CeWO_x$ surface at 200 °C.

3.5. Effect of SO_2 on NO adsorption

Firstly, the adsorption of NO on fresh $CeWO_x$ and SO_2-pretreated $CeWO_x$ was studied. As shown in Fig. 5, the amount of NO adsorbed at

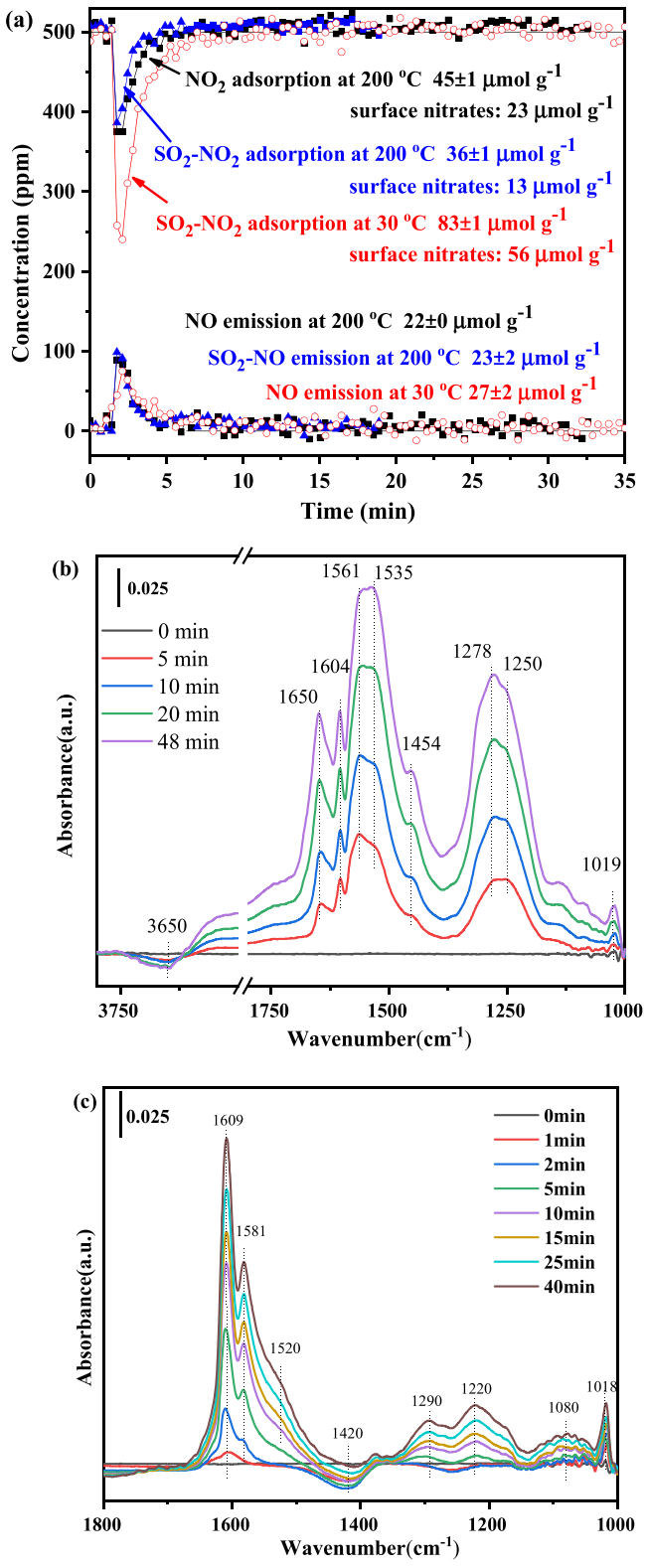

Fig. 3. NO_2/N_2 (500 ppm) adsorption on fresh $CeWO_x$ at 200 °C and on $CeWO_x$ saturated by SO_2/N_2 (100 ppm) at 30 and 200 °C (a); In situ DRIFTS of $CeWO_x$ treated in flowing 100 ppm SO_2 in N_2 until saturation, and then in 500 ppm NO_2 in N_2 at 30 °C (b) and at 200 °C (c).

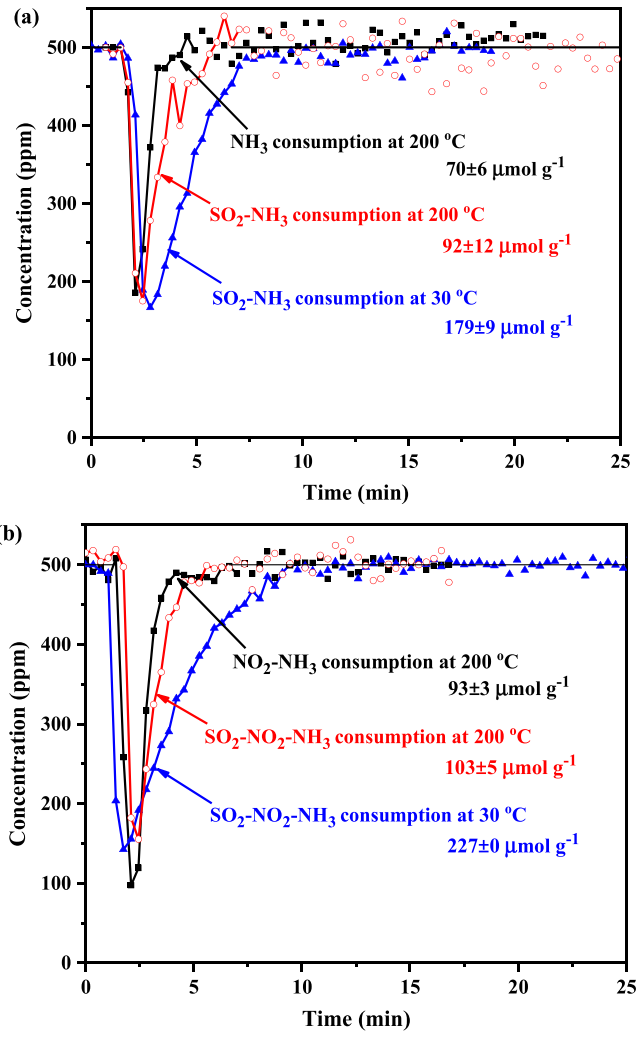

Fig. 4. NH_3/N_2 (500 ppm) adsorption on fresh $CeWO_x$ at 200 °C and on $CeWO_x$ saturated by SO_2/N_2 (100 ppm) at 30 and 200 °C (a); NH_3/N_2 (500 ppm) adsorption on $CeWO_x$ saturated by NO_2/N_2 (500 ppm) at 200 °C and on $CeWO_x$ saturated first by SO_2/N_2 (100 ppm) and then by NO_2/N_2 (500 ppm) at 30 and 200 °C (b).

30 °C on the SO_2-pretreated catalyst was ~8 μmol g^{-1}, which was less than that on the fresh catalyst (~10 μmol g^{-1}) [25]. This phenomenon may be due to the presence of some adsorbed SO_2 occupying the adsorption sites (Eqs. (1)–(2)). Similarly, competitive adsorption between NO and SO_2 was found on $Ce_{0.3}TiO_x$ [11] and V_2O_5-WO_3/TiO_2 [39]. The adsorption of NO might follow Eqs. (14), (15) and (4) [25]. At 200 °C, ~5 μmol g^{-1} NO was consumed and ~4 μmol g^{-1} NO_2 was produced on fresh $CeWO_x$ (Fig. 5), indicating that Eq. (13) may occur. This phenomenon does not exist at 150 °C [25]. The consumption of NO was ~3 μmol g^{-1} at 200 °C after SO_2 adsorption, indicating that the sulfate and sulfite species inhibited the oxidation of NO. Zhang et al. [11] also reported the competitive adsorption between SO_2 and NO and the inhibition of nitrate production from NO adsorption by SO_2 on $Ce_{0.3}TiO_x$.

$$[Ce^{4+}]\text{-}O^- + NO \leftrightarrow [Ce^{3+}]\text{-}\square + NO_2 \quad (13)$$

$$[Ce^{4+}]\text{-}O^- + NO \leftrightarrow [Ce^{4+}]\text{-}ONO \quad (14)$$

$$[Ce^{4+}]\text{-}ONO + [Ce^{4+}]\text{-}O^- \leftrightarrow ([Ce^{4+}]\text{-}O)_2 = NO \quad (15)$$

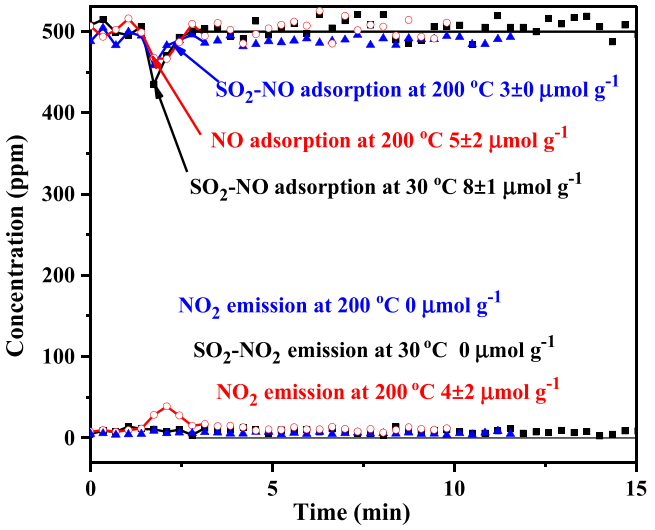

Fig. 5. NO/N_2 (500 ppm) adsorption on fresh $CeWO_x$ at 200 °C and on $CeWO_x$ saturated by SO_2/N_2 (100 ppm) at 30 and 200 °C.

3.6. Reaction between NO and adsorbed NH_3 after SO_2 and NO_2 adsorption

After the $CeWO_x$ was firstly saturated by SO_2, by NO_2 subsequently and then by NH_3 at 30 °C, NO was fed into the reactor and the consumption was ~0 μmol g^{-1} (Fig. 6**a**). Subsequently, TPSR was performed to study the reaction mechanism, and the results are shown in Fig. 6**b**. The emission of SO_2 was not observed during TPSR, indicating that the sulfate or sulfite species are stable and remain on the catalyst surface below 400 °C. The SO_2-TPD (Fig. S5) results confirm that sulfate/sulfite is stable below 400 °C and starts to desorb at 550 °C. Analogously, Zheng et al. found that adsorbed SO_2 would desorb above 500 °C on VMo/Ti-Si-Ce [40]. As shown in Fig. 6**b**, NO started to be consumed at about 100 °C and maximum consumption appeared at ~145 °C, shifting towards higher temperature compared with $CeWO_x$ without SO_2 adsorption (~115 °C) [25], indicating that sulfate and sulfite species can hinder the SCR reaction. As shown in Fig. 6**b**, ~38 μmol g^{-1} unreactive NH_3 desorption could be observed while there was no desorption of NH_3 from $CeWO_x$ without pre-adsorption of SO_2 [25], which indicated that some NH_3 became weakly adsorbed and could not participate in the SCR reaction. ~44 μmol g^{-1} NH_4NO_3 and ~23 μmol g^{-1} NH_4HSO_4 formed after adsorption of SO_2, NO_2 and NH_3. It can be calculated that the amount of adsorbed NH_3 (neither in the form of

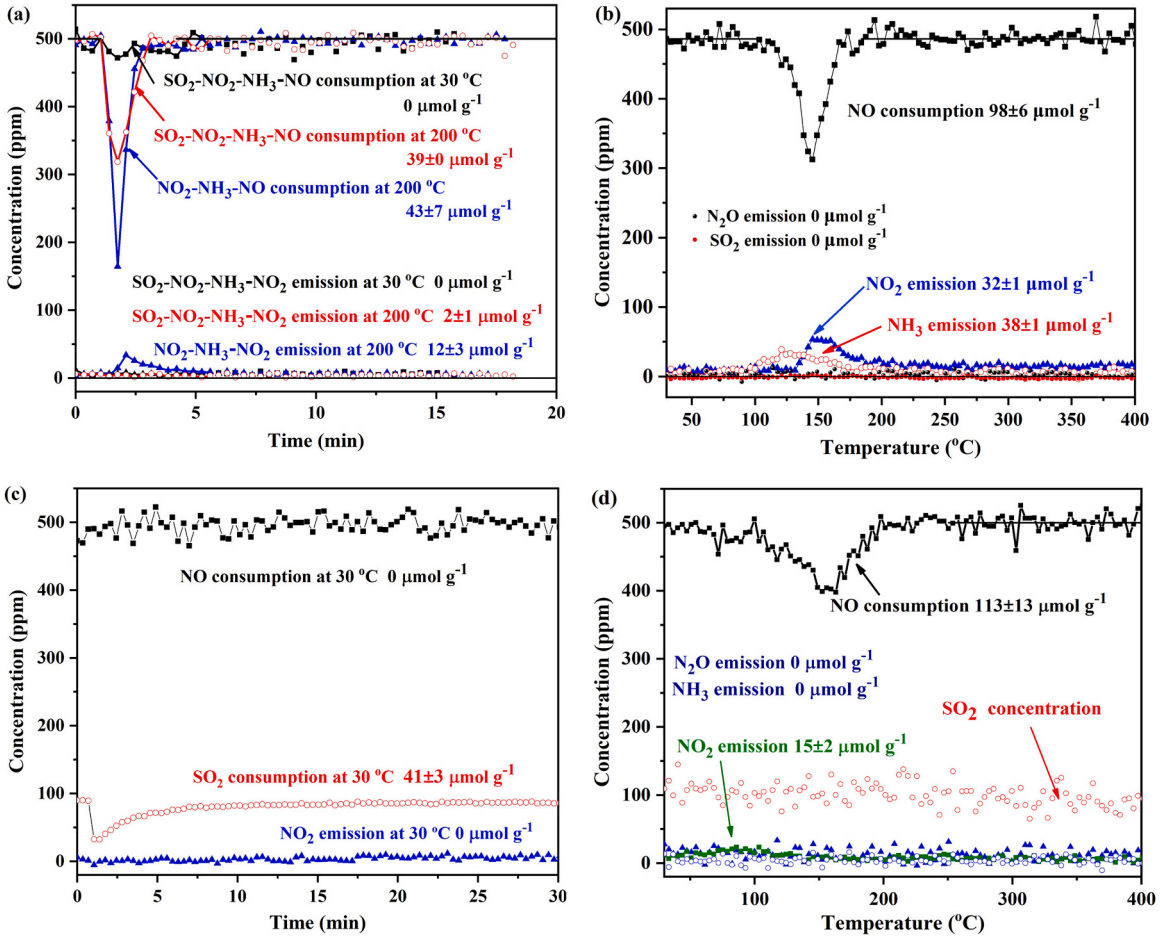

Fig. 6. (a) NO/N_2 (500 ppm) adsorption on $CeWO_x$ saturated firstly by NO_2/N_2 (500 ppm) and then by NH_3/N_2 (500 ppm) at 200 °C and on $CeWO_x$ saturated first by SO_2/N_2 (100 ppm) and then by NO_2/N_2 (500 ppm) and subsequently by NH_3/N_2 (500 ppm) at 30 and 200 °C; (b) TPSR in NO/N_2 (500 ppm) of $CeWO_x$ saturated first by SO_2/N_2 (100 ppm) and then by NO_2/N_2 (500 ppm) and subsequently by NH_3/N_2 (500 ppm) at 30 °C; (c) (500 ppm NO + 100 ppm SO_2)/N_2 adsorption and (d) TPSR in (500 ppm NO + 100 ppm SO_2)/N_2 on $CeWO_x$ saturated first by NO_2/N_2 (500 ppm) and then by NH_3/N_2 (500 ppm) at 30 °C.

Table 1
Reaction pathways under different experimental conditions.

Reactions		Numbers (μmol g^{-1})				
		TPSR1	TRM1	TRM2	TPSR2	TPSR3
$[M^{n+}]$-O-NH_4NO_3-$[Ce^{4+}]$ + NO→H_2O + N_2 + NO_2 + $[M^{n+}]$-OH + $[Ce^{4+}]$-OH	NH_4NO_3 path	32	12	2	15	0
NO + adsorbed NO_2 + 2(adsorbed NH_3) → $2N_2$ + $3H_2O$		12	11	11	45	30
$[Ce^{4+}]$-ONO + $[M^{n+}]$-NH_3 → H_2O + N_2 + $[Ce^{4+}]$-OH + $[M^{n+}][Ce^{4+}]$-ONO + $[M^{n+}]$-O-NH_4 → H_2O + N_2 + $[Ce^{4+}]$-OH + $[M^{n+}]$-OH	Nitrite path	31	19	6	53	71
$[Ce^{4+}]$-O^- + NO + NH_4HSO_4 → N_2 + $2H_2O$ + $[Ce^{4+}]$-HSO_4^-	Sulfate path	23	0	19		
NH_4NO_3 → N_2O + $2H_2O$		0	0	0	0	30

Note: TPSR1: TPSR of the SO_2-NO_2-NH_3 pretreated $CeWO_x$ in 500 ppm NO/N_2; TRM1: transient response experiment of the NO_2-NH_3 pretreated $CeWO_x$ in 500 ppm NO/N_2 at 200 °C; TRM2: transient response experiment of the SO_2-NO_2-NH_3 pretreated $CeWO_x$ in 500 ppm NO/N_2 at 200 °C; TPSR2: TPSR of $CeWO_x$ in NO + SO_2 after adsorption of NO_2 and NH_3 at 30 °C; TPSR3: TPSR of $CeWO_x$ in NO + SO_2 + H_2O after adsorption of NO_2 and NH_3 at 30 °C.

NH_4NO_3 nor NH_4HSO_4) that participated in TPSR was 227 - 78 - 38 - 44 - 23 = 44 μmol g^{-1}. The amounts of the consumed NO and produced NO_2 during TPSR were ~98 μmol g^{-1} and ~32 μmol g^{-1}, respectively (Fig. 6**b**). Therefore, ~98 μmol g^{-1} NO could react with ~44 μmol g^{-1} NH_4NO_3, ~23 μmol g^{-1} NH_4HSO_4 and 44 μmol g^{-1} adsorbed NH_3 to form H_2O, N_2 and ~32 μmol g^{-1} NO_{2H2O} and N . Also, it was reported that NO can react with NH_4^+ in NH_4HSO_4 to form H_2NNO, which will decompose into H_2O and N_2, and finally sulfate and sulfite species remain on the surface of catalyst [4]. Therefore, it can be concluded that during the TPSR process (TPSR1 in Table 1), 32 μmol g^{-1} NO reacted with surface NH_4NO_3 to produce H_2O, NO_2 and N_2 (Eq. (16)), 12 μmol g^{-1} NO reacted with 12 μmol g^{-1} nitrates and 24 μmol g^{-1} adsorbed NH_3 (Eq. (17)), 31 μmol g^{-1} NO reacted with 31 μmol g^{-1} adsorbed NH_3 to produce N_2 and H_2O (Eqs. (18)-(19)), and 23 μmol g^{-1} NO reacted with NH_4HSO_4 to form N_2, H_2O and HSO_4^- species according to Eq. (20) (the "sulfate path", which accounts for about 23% of the whole reaction). Based on our calculation, the following reactions took place:

$$[M^{n+}]\text{-O-}NH_4NO_3\text{-}[Ce^{4+}] + NO \rightarrow H_2O + N_2 + NO_2 + [M^{n+}]\text{-OH} + [Ce^{4+}]\text{-OH}\ \text{“}NH_4NO_3\ \text{path”} \quad (16)$$

$$NO + \text{adsorbed } NO_2 + 2(\text{adsorbed } NH_3) \rightarrow 2N_2 + 3H_2O \quad (17)$$

$$[Ce^{4+}]\text{-ONO} + [M^{n+}]\text{-}NH_3 \rightarrow H_2O + N_2 + [Ce^{4+}]\text{-OH} + [M^{n+}]\ \text{“nitrite path”} \quad (18)$$

$$[Ce^{4+}]\text{-ONO} + [M^{n+}]\text{-O-}NH_4 \rightarrow H_2O + N_2 + [Ce^{4+}]\text{-OH} + [M^{n+}]\text{-OH “nitrite path”} \quad (19)$$

$$[Ce^{4+}]\text{-}O^- + NO + NH_4HSO_4 \rightarrow N_2 + 2H_2O + [Ce^{4+}]\text{-}HSO_4^-\ \text{“sulfate path”} \quad (20)$$

where $[Ce^{4+}]$-ONO was mainly from adsorption of NO during standard SCR.

At 200 °C, reactions (16)-(19) took place without the SO_2 pretreatment (TRM1, Table 1). The reaction pathway consisted of the “nitrite path” and “NH_4NO_3 path”, which was quite similar to that at 150 °C [25], indicating that raising the temperature to 200 °C did not change the reaction mechanism on $CeWO_x$. At 200 °C, on the SO_2-NO_2-NH_3 pretreated $CeWO_x$, reactions (18)-(20) took place (TRM2, Table 1). In comparison with the catalyst without SO_2 pretreatment, the NO_2 formation was reduced, indicating that less nitrate participated in reaction (16). All of the ammonia bisulfate can be consumed at 200 °C. Moreover, the band ascribed to ammonia species vanished within 5 min in the in situ DRIFTspectra (Fig. S6c), indicating that ammonia bisulfate on the catalyst surface could be consumed after NO was introduced at 200 °C. The number of NH_3 species formed on Lewis and Brønsted acid sites on $CeWO_x$ at 200 °C was quantitatively determined after SO_2 and NO_2 treatment by pyridine-chemisorbed FTIR and TRM (Table S1). The surface was mostly covered by NH_3 on Brønsted acid sites (35 μmol g^{-1}), including 19 μmol g^{-1} NH_4HSO_4, 13 μmol g^{-1} NH_4NO_3, and 3 μmol g^{-1} $[M^{n+}]$-O-NH_4. According to Fig. S7, the NH_3 consumption by NO was faster on Brønsted acid sites than on Lewis acid sites at the initial stage (within 1 min), indicating that the Brønsted acid sites are more active than Lewis acid sites for NH_3-SCR. Also, the amount of NH_3 on Brønsted acid sites exceeded that on Lewis acid sites, demonstrating that Brønsted acid sites might make the main contribution during the reaction in the presence of SO_2. Similarly, it was reported that NO can react with NH_4HSO_4 on V_2O_5/TiO_2 at 200 °C and the reaction between NH_4HSO_4 and NO mainly begins at ~190 °C on 5 wt% V_2O_5/AC [41]. Song et al. [26] also found that NH_4HSO_4 can partly decompose on CeO_2 below 220 °C. Different from previous report [13], NH_4HSO_4 can be consumed completely by NO within 5 min at 200 °C on $CeWO_x$ (Fig. S6), indicating that the formation of NH_4HSO_4 might not be a key factor in the decrease in activity on $CeWO_x$. It should be noted that the higher amount of NH_3

adsorption should be beneficial for NH_3-SCR. However, decreased activity was observed (Fig. 1) and was not caused by NH_3 oxidation (Fig. S1c). In our previous study [42], it was found that NO adsorption is very important for standard SCR. Seen from Fig. 5, the amount of NO adsorption decreased after $CeWO_x$ was pretreated by SO_2, leading to the lower NH_3-SCR activity. In addition, the generated sulfate reduces the catalyst's ability to activate NO [8,11]. The reasons above led to a serious decrease in the activity during standard SCR at 200 °C.

Fig. 6**c** and **d** depicts the adsorption of NO + SO_2 and the temperature programmed surface reaction (TPSR) of $CeWO_x$ in NO + SO_2 after adsorption of NO_2 and NH_3 at 30 °C. No N_2O or NH_3 was released during the TPSR process. Seen from Table 1, reactions (16)-(20) took place (TPSR2). Similar to the TPSR result with NO only [25], the NO consumption could begin below 100 °C and reached a maximum consumption rate at ~150 °C. In comparison with the data in Fig. 6**b**, the temperature of the consumption peak in Fig. 6**d** is similar, indicating that SO_2 gas has no significant inhibitory effect on NH_3-SCR, and that the adsorbed SO_2 on the surface made the main contribution to the inhibitory effect. In the presence of SO_2, NO_2 was evolved at lower temperature (below 100 °C) in comparison with the TPSR in NO [25], and the amount of NO_2 emission was lower in the presence of SO_2, demonstrating that more nitrates formed from NO_2 adsorption participated in the NH_3-SCR reaction. Thus, it can be concluded that SO_2 facilitated the reaction between nitrates, adsorbed NH_3 and NO to form H_2O and N_2 (Eq. (17)) at low temperatures. In situ DRIFTS results show that the ammonia species on the $CeWO_x$ surface were consumed completely within 2 min when NO_2 was present (fast SCR), either in the presence or absence of SO_2 (Fig. S6a and **e**). According to the previous report [2], adsorbed NH_3 can be consumed completely by NO+O_2 at 200 °C within 3 min. However, adsorbed ammonia species remained after 60 min exposure to NO on $CeWO_x$ pretreated by SO_2 (Fig. S6b), indicating that the reaction between adsorbed NH_3 and NO was inhibited by SO_2 at 200 °C (Fig. 1). After pre-absorption of SO_2, NH_3 and NO_2 (Fig. S6c), the adsorbed ammonia species disappeared quickly when NO was introduced, indicating that NO_2 accelerated NH_3-SCR through the formation of surface nitrates. It was reported that sulfuric acid can reduce the decomposition temperature of NH_4NO_3 by replacing NO_3^- to form NH_4HSO_4 (Eq. (21)) [43].

$$NH_4NO_3 + H_2SO_4 \leftrightarrow NH_4HSO_4 + HNO_3 \quad (21)$$

Therefore, the produced HNO_3 could react with NO to produce nitrites, which would react with adsorbed NH_3 to produce H_2O and N_2 (Eqs. (18), (19), (22) and (23)).

$$HNO_3 + NO + Ce^{3+}\text{-}\square \leftrightarrow HNO_2 + Ce^{4+}\text{-}ONO \quad (22)$$

$$HNO_2 + NH_3 \rightarrow N_2 + 2H_2O \quad (23)$$

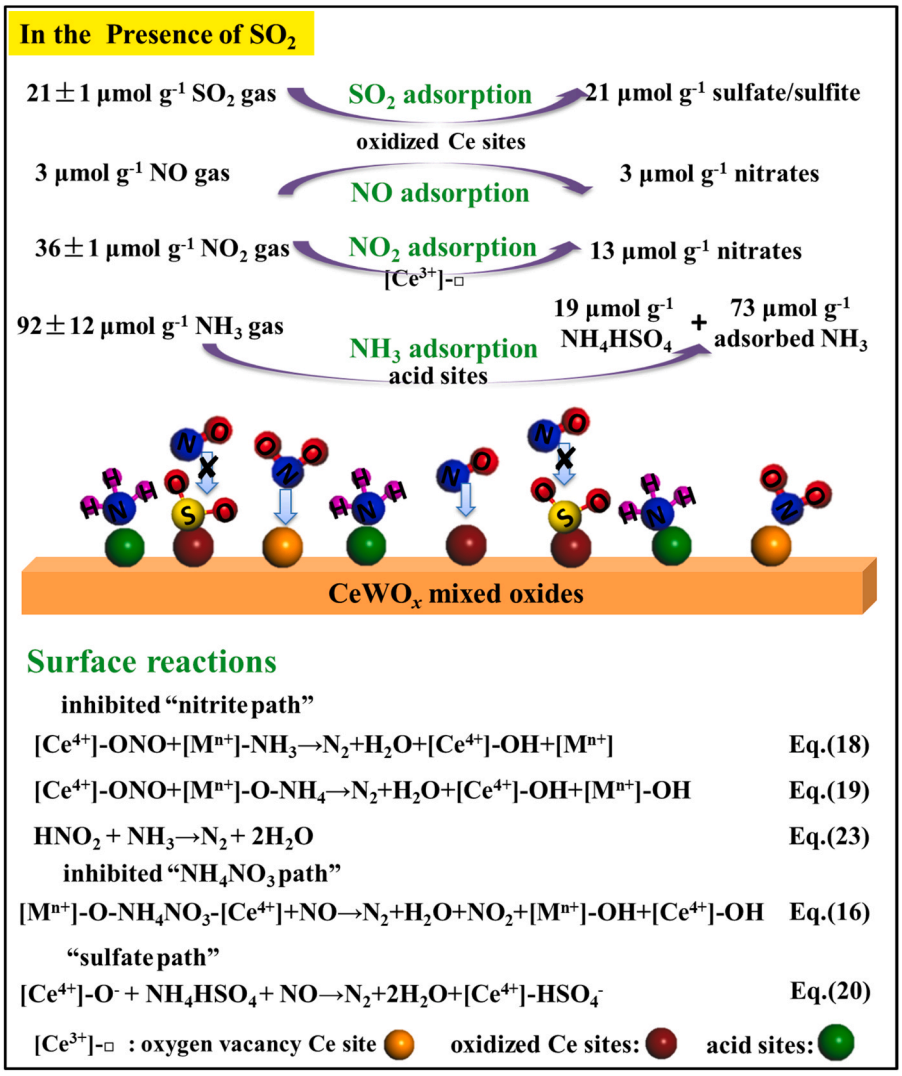

Fig. 7. NH_3-SCR mechanism on $CeWO_x$ in the presence of SO_2 at 200 °C.

NO adsorption was inhibited by SO_2 during standard SCR, leading to low NH_3-SCR activity. On the contrary, nitrates could also be produced from the adsorption of NO_2, and reactions (21)-(23) were promoted in the presence of SO_2 as discussed above; thus, the inhibitory effect of SO_2 during fast SCR was not as severe as that during standard SCR (Fig. 1). More NH_3 participated in NH_3-SCR during TPSR when SO_2 gas was present (Fig. 6**d**) since the reaction between SO_2 gas and surface NH_3 to form NH_4HSO_4 stabilized the adsorbed NH_3, and NH_4HSO_4 could react with NO gas to produce $[Ce^{4+}]$-HSO_4^-, H_2O and N_2 (Eq. (20)), leading to a lack of NH_3 desorption from the catalyst surface during TPSR.

According to the above results, the reaction pathways of SCR after adsorption of SO_2 include the "nitrite path", "NH_4NO_3 path" and "sulfate path" (Fig. 7). During standard SCR, SO_2 mainly occupies the oxidized Ce sites, and NO adsorption is prohibited by SO_2. The "nitrite path" was found to make the main contribution to standard SCR on $CeWO_x$ in the absence of SO_2 and H_2O [42]. In this study, the "NH_4NO_3 path" might contribute insignificantly during standard SCR since the amount of nitrates produced from NO adsorption was too small. The reaction pathway of standard SCR with SO_2 included "nitrite path" and "sulfate path". When SO_2 was present, the maximum consumption temperature of NO moved to higher temperature in the TPSR process (Fig. 6**b, d**), demonstrating that the "nitrite path" was inhibited in the presence of SO_2. All the factors above led to low NH_3-SCR activity during standard SCR at low temperatures (Fig. 1). The reaction pathway of fast SCR with SO_2 included the "nitrite path", "NH_4NO_3 path" and "sulfate path". During fast SCR, besides the inhibition of the "nitrite path", the lower NO_2 release during TPSR also indicated that the "NH_4NO_3 path" was inhibited at the same time. The sulfate and sulfite species inhibit the formation of nitrate and nitrites and weaken the adsorption of part of nitrate so that it cannot participate in the reaction. It was found that [6] the larger amount of SO_4^{2-} caused worse resistance to SO_2 poisoning on 4 V/TiO_2 and 4V6Mo/TiO_2. Therefore, it can be inferred that SO_4^{2-} contributed to the most important deactivation. However, the presence of NO_2 led to a higher concentration of surface nitrates than standard SCR, and more HNO_3 took part in reactions (21)-(23) to produce H_2O and N_2 in the presence of SO_2. It is reported that in standard SCR, the rate-determining step during the reaction between NO/O_2 and NH_4HSO_4 on the V_2O_5/TiO_2 catalyst is the reoxidation of reduced vanadium sites, and NO_2 has stronger oxidation ability than O_2, and thus, it can accelerate the decomposition of ammonium bisulfate [4]. Some researchers [44,45] found that the formation of bidentate nitrate could improve the sulfur resistance of the NH_3-SCR catalyst. In our study, in

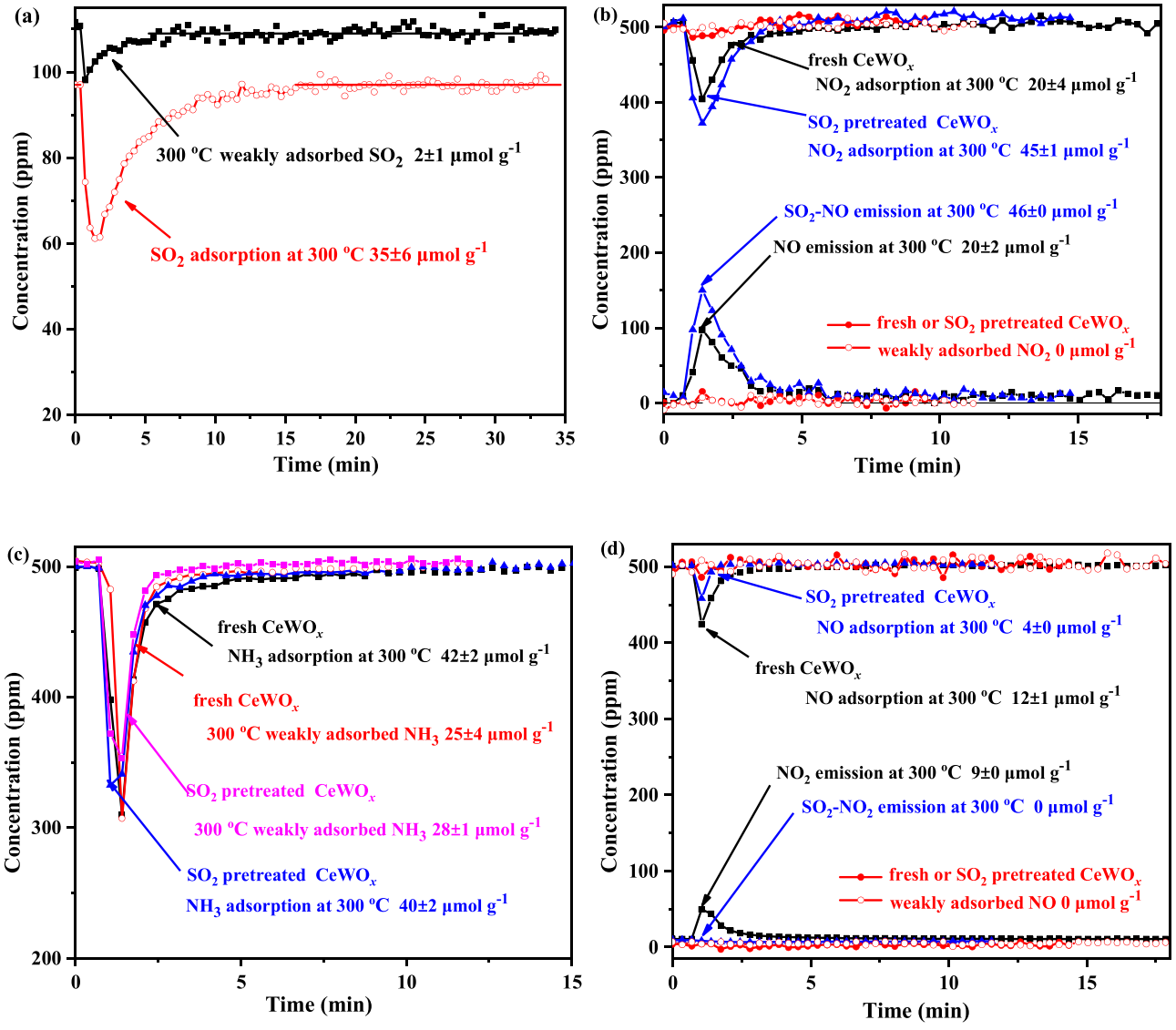

Fig. 8. (a) SO_2 adsorption on fresh $CeWO_x$ at 300 °C; (b) NO_2, (c) NH_3 and (d) NO adsorption on fresh $CeWO_x$ and on $CeWO_x$ pretreated by SO_2/N_2 at 300 °C. SO_2 concentration: 100 ppm; NO or NO_2 or NH_3 concentration: 500 ppm.

situ DRIFTS results show that the presence of NO_2 increased the formation of bidentate nitrate (Fig. S6) and accelerated the decomposition of ammonium bisulfate, possibly also because of the stronger oxidation ability of NO_2 than O_2 [4], which may be the reason for the better activity of fast SCR. Thus, although the "nitrite path" and "NH_4NO_3 path" were inhibited, the greater amount of nitrates formed from NO_2 adsorption, the acceleration of ammonium bisulfate decomposition, and the promoted reaction between NO gas, surface HNO_3 and adsorbed NH_3 (Eqs. (21)-(23)) result in the inhibitory effect of SO_2 during fast SCR being less severe than that during standard SCR (Fig. 1).

At higher temperatures, e.g. at 300 °C, the NO_x conversion decreased slightly in the presence of SO_2 under dry conditions after standard SCR for 4 h (Fig. 1**a**). Therefore, the inhibitory effect of SO_2 on NO adsorption and "nitrite path" might not be a key factor. As shown in Fig. 8**a**, the adsorption amount of SO_2 (~35 μmol g^{-1}) was greater at 300 °C than at 200 °C, possibly due to the oxidation of SO_2 at higher temperatures [46]. Interestingly, the amount of NO_2 consumption is similar to that of NO emission either in the presence or absence of SO_2 (Fig. 8**b**). Thus, it can be proposed that NO_2 played the role of oxidizing the sites on $CeWO_x$ at higher temperatures (reverse reaction (13)) [4]. The amount of NO_2 consumption was higher on the SO_2 pretreated $CeWO_x$ due to Reaction (10). However, the pre-adsorbed SO_2 did not increase the amount of NH_3 adsorption at 300 °C (Fig. 8**c**), indicating that the acidity sites were not increased by the pre-adsorbed SO_2 and NH_4HSO_4 or $(NH_4)_2SO_4$ was not generated at 300 °C. An explanation for this phenomenon is that NH_4HSO_4 or $(NH_4)_2SO_4$ decomposed to adsorbed ammonia and sulfate below 300 °C [26]. Thus, "sulfate path" was absent at 300 °C. Greater amount of NO consumption was observed at 300 °C than at 200 °C due to NO oxidation to NO_2 on fresh $CeWO_x$ (Fig. 8**d**). However, no NO_2 was generated on the SO_2 pre-adsorbed catalyst, indicating that sulfate inhibited NO oxidation. Considering the extremely small amount of NO adsorption (Fig. 8**d**), it can be suggested that the Eley-Rideal (E-R) mechanism (adsorbed NH_3 reacting with gaseous NO to N_2 and H_2O) contributed mainly to standard SCR at 300 °C. However, at 200 °C, the mechanism might be different. According to our previous study [43], L-H mechanism ("nitrite path") contributed mainly to standard SCR in the absence of SO_2 on $CeWO_x$. In this study, nitrates were produced on the SO_2 pretreated $CeWO_x$ after NO adsorption at 200 °C (Fig. S8), indicating that NO could adsorb on the SO_2 pretreated $CeWO_x$ catalyst, although the amount of NO adsorption is small. Therefore, L-H mechanism is present at 200 °C in the presence of SO_2. Nevertheless, since the amount of NO adsorption was low, E-R mechanism cannot be excluded in the presence of SO_2. Similar to $Ce_{0.3}TiO_x$ [11], E-R mechanism made the main contribution at high temperatures while L-H mechanism was important at low temperatures during standard SCR on $CeWO_x$.

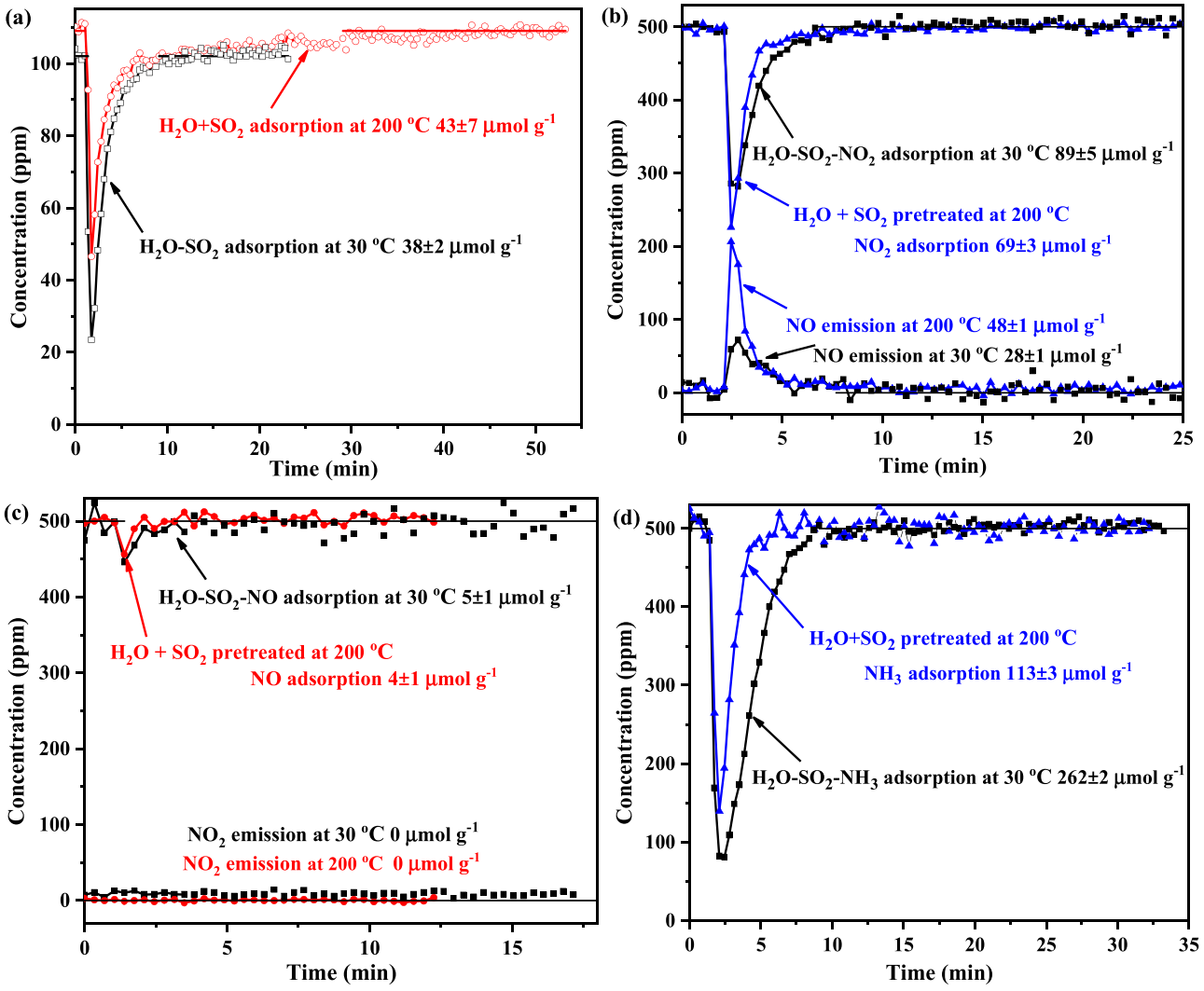

Fig. 9. (a) SO_2 adsorption on H_2O-pretreated $CeWO_x$ (H_2O-SO_2) at 30 °C, SO_2 and H_2O co-adsorption on fresh $CeWO_x$ (H_2O+SO_2) at 200 °C; (b) NO_2, (c) NO and (d) NH_3 adsorption on $CeWO_x$ pretreated first with H_2O and then SO_2 at 30 °C and on $CeWO_x$ pretreated with (H_2O+SO_2) at 200 °C. SO_2 concentration: 100 ppm, H_2O concentration: 2 vol%, NO or NO_2 or NH_3 concentration: 500 ppm.

3.7. NH_3-SCR reaction mechanism in the presence of SO_2 and H_2O

When SO_2 and H_2O are present at the same time, the reaction activity is seriously inhibited at 200 °C. Therefore, the effect of SO_2 and H_2O on the adsorption amounts of NO_2, NH_3, NO and the NH_3-SCR mechanism on $CeWO_x$ was comprehensively investigated. After pre-adsorption of H_2O, the consumption of SO_2 was ~38 μmol g^{-1} at 30 °C (Fig. 9**a**), while the amount of weakly adsorbed SO_2 molecules was ~7 μmol g^{-1} (Fig. S2). At 200 °C, as seen in Fig. 9**a**, when 100 ppm SO_2 and 2 vol% H_2O were present at the same time, the consumption of SO_2 was ~43 μmol g^{-1} and there were no weakly adsorbed SO_2 molecules (Fig. S2). The SO_2 consumption was higher than that without water, indicating that more sulfate and sulfite species were produced when water was present, and SO_2 can react with H_2O on the catalyst surface [30] through Eq. (24).

$$SO_2 + H_2O \leftrightarrow HSO_3^- + H^+ \leftrightarrow SO_3^{2-} + 2H^+ \quad (24)$$

As shown in Fig. 9**b**, after adsorption of H_2O and SO_2, the NO_2 consumption was ~89 μmol g^{-1} and the NO emission was ~28 μmol g^{-1} at 30 °C. The amounts are similar to those on the SO_2-pretreated catalyst. The molecular ratio of NO_2 to NO was about 3:1. The existence of SO_2 does not affect the adsorption pathway of NO_2, which may follow Eq. (7) [25]. However, the consumption of NO_2 and NO formation were ~69 μmol g^{-1} and ~48 μmol g^{-1} after 2 vol% H_2O and SO_2 pretreatment at 200 °C (Fig. 9**b**), respectively, and both were higher than on the SO_2 pre-adsorbed $CeWO_x$. NO evolution was due to reactions (5) [25] and (10). Large amounts of NO evolved during NO_2 adsorption, indicating that more adsorbed SO_2 on $CeWO_x$ led to more NO_2 participating in Reaction (10), emitting more NO gas.

The consumption of NO was ~5 μmol g^{-1} and ~4 μmol g^{-1} after adsorption of H_2O and SO_2 at 30 °C and after adsorption of H_2O and SO_2 at 200 °C, respectively (Fig. 9**c**), while the NO consumption was ~8 μmol g^{-1} (Fig. 5) at 30 °C on SO_2-pretreated $CeWO_x$, indicating that the combined effect of H_2O and SO_2 decreased the NO adsorption amount further in comparison with the results in the presence of only SO_2. NO adsorption has been considered to be an important process for obtaining high standard SCR activity [47], and the decrease in NO adsorption led to lower SCR activity (Fig. 1). H_2O aggravated the inhibitory effect of SO_2 on NO adsorption, possibly due to the increased amounts of adsorbed sulfate and sulfite species (Fig. 9**a**).

As seen in Fig. 9**d**, the amount of NH_3 consumption after pretreatment by H_2O and SO_2 was ~262 μmol g^{-1} at 30 °C, 17 μmol g^{-1} and 83 μmol g^{-1} higher than that when only H_2O [25] or SO_2 (Fig. 4**a**) was present, respectively. The presence of H_2O could increase the amount of NH_3 adsorbed. As shown in Section 3.2, ~23 μmol g^{-1} sulfate and sulfite species were formed after SO_2 adsorption. After pre-adsorption of H_2O, ~31 μmol g^{-1} sulfate/sulfite species were on the surface, 8 μmol g^{-1} more than that on fresh $CeWO_x$. Wang et al. proposed that NH_4HSO_4 is more stable, viscous and corrosive, and more easily adsorbed on the catalyst surface [4]. Tang et al. pointed out that the formation temperature of NH_4HSO_4 is in the range of about 190–240 °C over vanadium-based catalysts [38]. Therefore, it is speculated that SO_2 increased NH_3 adsorption by 31 μmol g^{-1} and H_2O increased NH_3 adsorption by 262 - 160 - 31 = 71 μmol g^{-1}. At 200 °C, the consumption of NH_3 after pretreatment with H_2O and SO_2 was ~43 μmol g^{-1} higher than that of fresh $CeWO_x$ (Fig. 4**a**, ~70 μmol g^{-1}), exactly equal to the amount of surface sulfate and sulfite species, indicating that ~43 μmol g^{-1} ammonium bisulfate was generated.

Fig. 10 depicts the adsorption of (H_2O + NO + SO_2) and the subsequent TPSR of $CeWO_x$ in (H_2O + NO + SO_2) after adsorption of NO_2 and NH_3 at 30 °C. After NO_2 and NH_3 adsorption on $CeWO_x$ at 30 °C, NO, SO_2 and H_2O were introduced at the same time, and the consumption of NO was ~0 μmol g^{-1}. As shown in Fig. 10**b**, during the TPSR process, the concentration of SO_2 gradually decreases with increasing temperature. SO_2 can react with CeO_2 to form ceric sulfate and the sulfation process

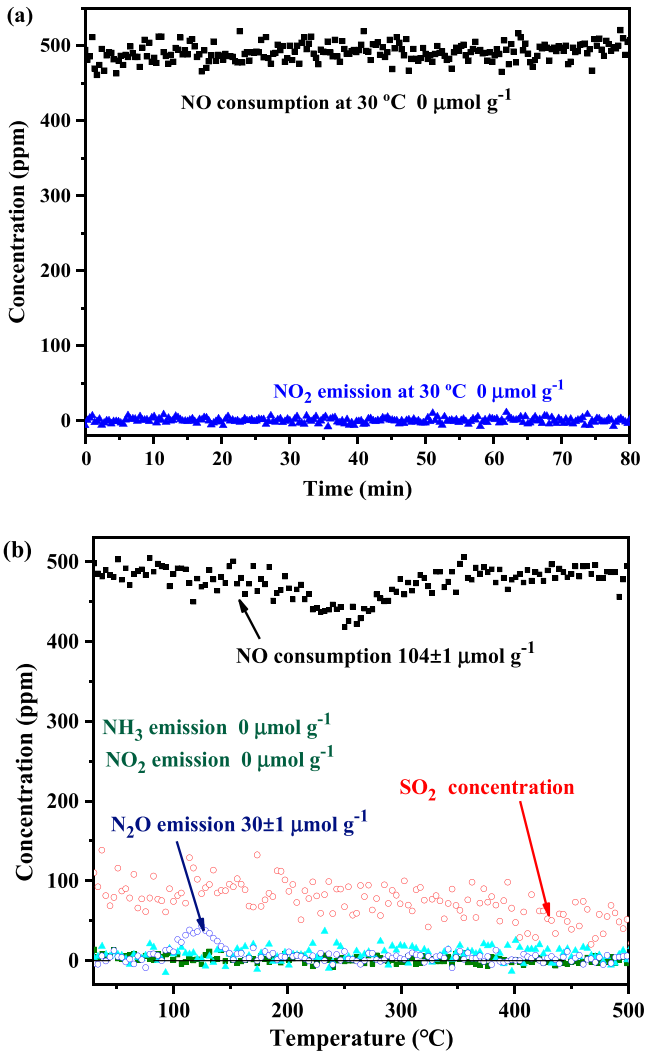

Fig. 10. (500 ppm NO + 2 vol% H_2O + 100 ppm SO_2)/N_2 adsorption (a) and TPSR in (500 ppm NO + 2 vol% H_2O + 100 ppm SO_2)/N_2 (b) on $CeWO_x$ saturated first by NO_2/N_2 (500 ppm) and then by NH_3/N_2 (500 ppm) at 30 °C.

gradually increases with rising temperature [46], causing a decrease in the SO_2 concentration. No formation of NH_3 or NO_2 was detected, while ~30 μmol g^{-1} N_2O was released. It is widely accepted that the NH_4NO_3 formed on NH_3-SCR catalysts, e.g. Cu-SSZ-13 [48], TiO_2-WO_3-V_2O_5 [49] and Fe-ZSM-5 [50], will decompose into N_2O through Eq. (25).

$$NH_4NO_3 \rightarrow N_2O + 2H_2O \quad (25)$$

However, in this study, the decomposition temperature of ammonium nitrate was below 150 °C, lower than values reported in the literature [48–50]. It can be proposed that H_2SO_4 formed from the reaction between H_2O and SO_2 lowered the decomposition temperature of NH_4NO_3 [43].

According to the TPSR results in Fig. 10**b**, it can be inferred that reactions (16)-(20) took place based on the calculation (TPSR3, Table 1 and Section S1.2). As seen from Fig. 10**b**, NO consumption can be observed in the temperature range from 190° to 350°C, and the consumption peak moves to higher temperature in comparison with that when only SO_2 was present (Fig. 6**d**). Therefore, it can be concluded that the reaction paths were prohibited by H_2O and SO_2. When H_2O and SO_2 were present simultaneously, the reaction pathways of NH_3-SCR included the "nitrite path", "sulfate path" and NH_4NO_3 decomposition to N_2O. The presence of H_2O changed the reaction pathways and the "NH_4NO_3 path" was absent. H_2O increased the formation of sulfate and

sulfite species, blocked the "NH_4NO_3 path" and inhibited the "nitrite path". For standard SCR, NO adsorption was more severely decreased with $H_2O + SO_2$ than with SO_2, and the "nitrite path" was inhibited, leading to a decrease in NO conversion to < 5% at 200 °C (Fig. 1). During fast SCR, even when nitrates were formed at 200 °C, the activity of fast SCR exhibited a dramatic decline. The reaction between NO and the surface nitrate and NH_3 species started at about 190 °C (Fig. 10**b**). Therefore, at the low temperature of 200 °C, it is difficult for the "nitrite path" and "NH_4NO_3 path" to take place, and the activity of fast SCR suffered a drastic decrease (Fig. 1).

4. Conclusions

In this study, the influence of SO_2 and the synergistic effect of H_2O and SO_2 on standard and fast SCR over $CeWO_x$ were explored in detail. The negative effect of SO_2 on fast SCR was less severe than on standard SCR. NH_4HSO_4 and sulfate/sulfite species could form during the reaction. NH_3 adsorbed on Brønsted acid sites is more active than that on Lewis acid sites and made the main contribution to SCR in the presence of SO_2. Ammonium bisulfate may not be the main cause of deactivation since it can be consumed completely by NO at 200 °C on $CeWO_x$. The sulfate and sulfite species inhibit NO adsorption and the formation of nitrate. At the same time, part of the NH_3 become weakly adsorbed and could not participate in the reaction. In situ DRIFTS results showed that when NO_2 is present, more bidentate nitrates can be generated and ammonia species have a faster consumption rate. This is a reason why fast SCR can maintain better activity. When only SO_2 is present, fast SCR follows the "nitrite path", "NH_4NO_3 path" and "sulfate path", and standard SCR follows the "nitrite path" and "sulfate path". During standard SCR, the "nitrite path" was inhibited, leading to a decrease in activity. However, during fast SCR, although the "nitrite path" and "NH_4NO_3 path" were inhibited, the greater amount of nitrates from NO_2 adsorption, acceleration of ammonium bisulfate decomposition, and the promoted reaction between surface HNO_3, adsorbed NH_3, and the NO gas alleviated the inhibitory effect of SO_2. At 300 °C, E-R mechanism (adsorbed NH_3 reacting with gaseous NO to N_2 and H_2O) contributed mainly to standard SCR and the mechanism is different from that at 200 °C. When both H_2O and SO_2 were present, more sulfate/sulfite was generated and NO adsorption as well as the "nitrite path" were further inhibited, causing more severely decreased activity for standard SCR. For fast SCR, the "nitrite path" was inhibited and the "NH_4NO_3 path" was blocked in the presence of H_2O and SO_2, leading to severe deactivation at low temperatures.

CRediT authorship contribution statement

Yanlong Huo: Data curation, Investigation, Formal analysis, Writing - original draft ， Writing - review & editing. **Kuo Liu**: Conceptualization, Methodology, Validation, Writing - review & editing, Project administration, Funding acquisition. **Jingjing Liu**: Data curation, Investigation, Validation. **Hong He**: Conceptualization, Writing - review & editing, Project administration, Resources, Supervision, Funding acquisition.

Declaration of Competing Interest

The authors declare that they have no known competing financial interests or personal relationships that could have appeared to influence the work reported in this paper.

Acknowledgements

This work was financially supported by the National Natural Science Foundation of China (21872168, 21637005, U20B6004).

Appendix A. Supporting information

Supplementary data associated with this article can be found in the online version at doi:10.1016/j.apcatb.2021.120784.

References

[1] L. Han, S. Cai, M. Gao, J.-Y. Hasegawa, P. Wang, J. Zhang, L. Shi, D. Zhang, Selective catalytic reduction of NO_x with NH_3 by using novel catalysts: state of the art and future prospects, Chem. Rev. 119 (2019) 10916–10976.
[2] W. Shan, F. Liu, H. He, X. Shi, C. Zhang, Novel cerium–tungsten mixed oxide catalyst for the selective catalytic reduction of NO_x with NH_3, Chem. Commun. 47 (2011) 8046–8048.
[3] J. Liu, G. He, W. Shan, Y. Yu, Y. Huo, Y. Zhang, M. Wang, R. Yu, S. Liu, H. He, Introducing tin to develop ternary metal oxides with excellent hydrothermal stability for NH_3 selective catalytic reduction of NO, Appl. Catal. B: Environ. 291 (2021), 120125.
[4] X. Wang, X. Du, S. Liu, G. Yang, Y. Chen, L. Zhang, X. Tu, Understanding the deposition and reaction mechanism of ammonium bisulfate on a vanadia SCR catalyst: a combined DFT and experimental study, Appl. Catal. B: Environ. 260 (2020), 118168.
[5] M.H. Zhu, J.K. Lai, U. Tumuluri, Z.L. Wu, I.E. Wachs, Nature of active sites and surface intermediates during SCR of NO with NH_3 by supported V_2O_5-WO_3/TiO_2 catalysts, J. Am. Chem. Soc. 139 (2017) 15624–15627.
[6] S. Zang, G. Zhang, W. Qiu, L. Song, R. Zhang, H. He, Resistance to SO_2 poisoning of V_2O_5/TiO_2-PILC catalyst for the selective catalytic reduction of NO by NH_3, Chin. J. Catal. 37 (2016) 888–897.
[7] M.N. Khan, L. Han, P. Wang, J. He, B. Yang, T. Yan, L. Shi, D. Zhang, SO_2-tolerant NO_x reduction over ceria-based catalysts: Shielding effects of hollandite Mn-Ti oxides, Chem. Eng. J. 397 (2020), 125535.
[8] L. Ma, C.Y. Seo, M. Nahata, X.Y. Chen, J.H. Li, J.W. Schwank, Shape dependence and sulfate promotion of CeO_2 for selective catalytic reduction of NO_x with NH_3, Appl. Catal. B: Environ. 232 (2018) 246–259.
[9] S.S. Liu, H. Wang, R.D. Zhang, Y. Wei, Synergistic effect of niobium and ceria on anatase for low-temperature NH_3-SCR of NO process, Mol. Catal. 478 (2019), 110563.
[10] Q. Yan, Y. Gao, Y. Li, M.A. Vasiliades, S. Chen, C. Zhang, R. Gui, Q. Wang, T. Zhu, A.M. Efstathiou, Promotional effect of Ce doping in $Cu_4Al_1O_x$–LDO catalyst for low-T practical NH_3-SCR: steady-state and transient kinetics studies, Appl. Catal. B: Environ. 255 (2019), 117749.
[11] Z. Zhang, L. Chen, Z. Li, P. Li, F. Yuan, X. Niu, Y. Zhu, Activity and SO_2 resistance of amorphous Ce_aTiO_x catalysts for the selective catalytic reduction of NO with NH_3: in situ DRIFT studies, Catal. Sci. Technol. 6 (2016) 7151–7162.
[12] X. Wang, X. Du, L. Zhang, G. Yang, Y. Chen, J. Ran, Simultaneous fast decomposition of NH_4HSO_4 and efficient NO_x removal by NO_2 addition: an option for NO_x removal in H_2O/SO_2-contained flue gas at a low temperature, Energy Fuels 32 (2018) 6990–6994.
[13] W. Xu, H. He, Y. Yu, Deactivation of a Ce/TiO_2 catalyst by SO_2 in the selective catalytic reduction of NO by NH_3, J. Phys. Chem. C 113 (2009) 4426–4432.
[14] M. Waqif, P. Bazin, O. Saur, J.C. Lavalley, G. Blanchard, O. Touret, Study of ceria sulfation, Appl. Catal. B: Environ. 11 (1997) 193–205.
[15] J.A. Rodriguez, T. Jirsak, S. Chaturvedi, J. Hrbek, Surface chemistry of SO_2 on Sn and Sn/Pt(111) alloys: effects of Metal−Metal bonding on reactivity toward sulfur, J. Am. Chem. Soc. 120 (1998) 11149–11157.
[16] M.Y. Smirnov, A.V. Kalinkin, A.V. Pashis, A.M. Sorokin, A.S. Noskov, V. I. Bukhtiyarov, K.C. Kharas, M.A. Rodkin, Comparative XPS study of Al_2O_3 and CeO_2 sulfation in reactions with SO_2, SO_2+O_2, SO_2+H_2O, and SO_2+O_2+H_2O, Kinet. Catal. 44 (2003) 575–582.
[17] E. Tronconi, I. Nova, C. Ciardelli, D. Chatterjee, M. Weibel, Redox features in the catalytic mechanism of the "standard" and "fast" NH_3-SCR of NO_x over a V-based catalyst investigated by dynamic methods, J. Catal. 245 (2007) 1–10.
[18] L. Cao, L. Chen, X.D. Wu, R. Ran, T.F. Xu, Z. Chen, D. Weng, TRA and DRIFTS studies of the fast SCR reaction over CeO_2/TiO_2 catalyst at low temperatures, Appl. Catal. A: Gen. 557 (2018) 46–54.
[19] Z. Chen, Z. Si, L. Cao, X. Wu, R. Ran, D. Weng, Decomposition behavior of ammonium nitrate on ceria catalysts and its role in the NH_3-SCR reaction, Catal. Sci. Technol. 7 (2017) 2531–2541.
[20] X. Wang, X. Du, L. Zhang, Y. Chen, G. Yang, J. Ran, Promotion of NH_4HSO_4 decomposition in NO/NO_2 contained atmosphere at low temperature over V_2O_5-WO_3/TiO_2 catalyst for NO reduction, Appl. Catal. A: Gen. 559 (2018) 112–121.
[21] Y. Inomata, S. Hata, M. Mino, E. Kiyonaga, K. Morita, K. Hikino, K. Yoshida, H. Kubota, T. Toyao, K. Shimizu, M. Haruta, T. Murayama, Bulk vanadium oxide versus conventional V_2O_5/TiO_2: NH_3-SCR catalysts working at a low temperature below 150 °C, ACS Catal. 9 (2019) 9327–9331.
[22] A. Marberger, D. Ferri, M. Elsener, O. Krocher, The significance of lewis acid sites for the selective catalytic reduction of nitric oxide on vanadium-based catalysts, Angew. Chem. Int. Ed. 55 (2016) 11989–11994.
[23] N.Y. Topsoe, Mechanism of the selective catalytic reducation of nitric-oxide by ammonia elucidated by in-situ online fourier transform infrared spectroscopy, Science 265 (1994) 1217–1219.
[24] Y. Inomata, H. Kubota, S. Hata, E. Kiyonaga, K. Morita, K. Yoshida, N. Sakaguchi, T. Toyao, K.-i Shimizu, S. Ishikawa, W. Ueda, M. Haruta, T. Murayama, Bulk tungsten-substituted vanadium oxide for low-temperature NO_x removal in the presence of water, Nat. Commun. 12 (2021) 557.

[25] K. Liu, H. He, Y. Yu, Z. Yan, W. Yang, W. Shan, Quantitative study of the NH_3-SCR pathway and the active site distribution over $CeWO_x$ at low temperatures, J. Catal. 369 (2019) 372–381.
[26] L.Y. Song, J.D. Chao, Y.J. Fang, H. He, J. Li, W.G. Qiu, G.Z. Zhang, Promotion of ceria for decomposition of ammonia bisulfate over V_2O_5-MoO_3/TiO_2 catalyst for selective catalytic reduction, Chem. Eng. J. 303 (2016) 275–281.
[27] B.Q. Jiang, Z.B. Wu, Y. Liu, S.C. Lee, W.K. Ho, DRIFT study of the SO_2 effect on low-temperature SCR reaction over Fe−Mn/TiO_2, J. Phys. Chem. C 114 (2010) 4961–4965.
[28] Q.X. Ma, Y.C. Liu, H. He, Synergistic effect between NO_2 and SO_2 in their adsorption and reaction on gamma-alumina, J. Phys. Chem. A 112 (2008) 6630–6635.
[29] S. Gao, P. Wang, F. Yu, H. Wang, Z. Wu, Dual resistance to alkali metals and SO_2: vanadium and cerium supported on sulfated zirconia as an efficient catalyst for NH_3-SCR, Catal. Sci. Technol. 6 (2016) 8148–8156.
[30] K. Hirota, J. Mäkelä, O. Tokunaga, Reactions of sulfur dioxide with ammonia: dependence on oxygen and nitric oxide, Ind. Eng. Chem. Res. 35 (1996) 3362–3368.
[31] A.L. Goodman, P. Li, C.R. Usher, V.H. Grassian, Heterogeneous uptake of sulfur dioxide on aluminum and magnesium oxide particles, J. Phys. Chem. A 105 (2001) 6109–6120.
[32] J.A. Rodriguez, T. Jirsak, A. Freitag, J.C. Hanson, J.Z. Larese, S. Chaturvedi, Interaction of SO_2 with CeO_2 and Cu/CeO_2 catalysts: photoemission, XANES and TPD studies, Catal. Lett. 62 (1999) 113–119.
[33] K. Liu, F. Liu, L. Xie, W. Shan, H. He, DRIFTS study of a Ce-W mixed oxide catalyst for the selective catalytic reduction of NO_x with NH_3, Catal. Sci. Technol. 5 (2015) 2290–2299.
[34] D. Meng, W. Zhan, Y. Guo, Y. Guo, L. Wang, G. Lu, A highly effective catalyst of Sm-MnO_x for the NH_3-SCR of NO_x at low temperature: promotional role of Sm and Its catalytic performance, ACS Catal. 5 (2015) 5973–5983.
[35] Y.H. Yeom, B. Wen, W.M.H. Sachtler, E. Weitz, NO_x reduction from diesel emissions over a nontransition metal zeolite catalyst: a mechanistic study Using FTIR spectroscopy, J. Phys. Chem. B 108 (2004) 5386–5404.
[36] J.O.L. Wendt, C.V. Sternling, Catalysis of SO_2 oxidation by nitrogen oxides, Combust. Flame 21 (1973) 387–390.
[37] S. Ma, M. Guo, H. Song, G. Chen, J. Yang, B. Zang, Z. Li, Formation mechanism and influencing factors of ammonium bissulfate during the selective catalytic reduction process, Therm. Power Genertion 43 (2014) 75–78.
[38] H. Tang, H. Li, J. Yang, Z. Lin, K. Zhuang, Q. Lu, W. Li, Research progress on the formation and decomposition mechanism of ammonium-sulfate salts in NH_3-SCR technology, Chem. Ind. Eng. Pro. 37 (2018) 822–831.
[39] Y. Liu, H. Shu, Q. Xu, Y. Zhang, L. Yang, FT-IR study of the catalytic oxidation of SO_2 during the process ofselective catalytic reduction of NO with NH_3 over commercial catalysts, J. Fuel Chem. Technol. 43 (2015) 1018–1024.
[40] C. Zheng, T. Cheng, L. Yang, H. Wu, H. Fan, Effect of SiO_2 addition on NH_4HSO_4 decomposition and SO_2 poisoning over V_2O_5-MoO_3/TiO_2-CeO_2 catalyst, J. Environ. Sci. 91 (2020) 279–291.
[41] Z.P. Zhu, H.X. Niu, Z.Y. Liu, S.J. Liu, Decomposition and reactivity of NH_4HSO_4 on V_2O_5/AC catalysts used for NO reduction with ammonia, J. Catal. 195 (2000) 268–278.
[42] K. Liu, H. He, B. Chu, Microkinetic study of NO oxidation, standard and fast NH_3-SCR on $CeWO_x$ at low temperatures, Chem. Eng. J. 423 (2021), 130128.
[43] Z. Sun, J. Sun, S. Lu, S. Shen, Study of the influence of inorganic acid on the thermal stability of ammonium nitrate, China Saf. Sci. J. 15 (2005) 57–62.
[44] F.Y. Gao, X.L. Tang, H.H. Yi, J.Y. Li, S.Z. Zhao, J.G. Wang, C. Chu, C.L. Li, Promotional mechanisms of activity and SO_2 tolerance of Co- or Ni-doped MnO_x-CeO_2 catalysts for SCR of NO_x with NH_3 at low temperature, Chem. Eng. J. 317 (2017) 20–31.
[45] X. Wang, R. Duan, W. Liu, D. Wang, B. Wang, Y. Xu, C. Niu, J.-W. Shi, The insight into the role of CeO_2 in improving low-temperature catalytic performance and SO_2 tolerance of $MnCoCeO_x$ microflowers for the NH_3-SCR of NO_x, Appl. Surf. Sci. 510 (2020), 145517.
[46] L. Zhang, W.X. Zou, K.L. Ma, Y. Cao, Y. Xiong, S.G. Wu, C.J. Tang, F. Gao, L. Dong, Sulfated temperature effects on the catalytic activity of CeO_2 in NH_3-selective catalytic reduction conditions, J. Phys. Chem. C 119 (2015) 1155–1163.
[47] K. Liu, Y.L. Huo, Z.D. Yan, W.P. Shan, H. He, Inhibitory role of excessive NH_3 in NH_3-SCR on $CeWO_x$ at low temperatures, Catal. Sci. Technol. 10 (2020) 2758–2762.
[48] Y. Shan, X. Shi, G. He, K. Liu, Z. Yan, Y. Yu, H. He, Effects of NO_2 addition on the NH_3-SCR over small-pore Cu-SSZ-13 zeolites with varying Cu loadings, J. Phys. Chem. C 122 (2018) 25948–25953.
[49] G. Madia, M. Koebel, M. Elsener, A. Wokaun, Side reactions in the selective catalytic reduction of NO_x with various NO_2 fractions, Ind. Eng. Chem. Res. 41 (2002) 4008–4015.
[50] M. Devadas, O. Kroecher, M. Elsener, A. Wokaun, N. Soeger, M. Pfeifer, Y. Demel, L. Mussmann, Influence of NO_2 on the selective catalytic reduction of NO with ammonia over Fe-ZSM5, Appl. Catal. B: Environ. 67 (2006) 187–196.